

# Control of Motorcycle Steering Instabilities

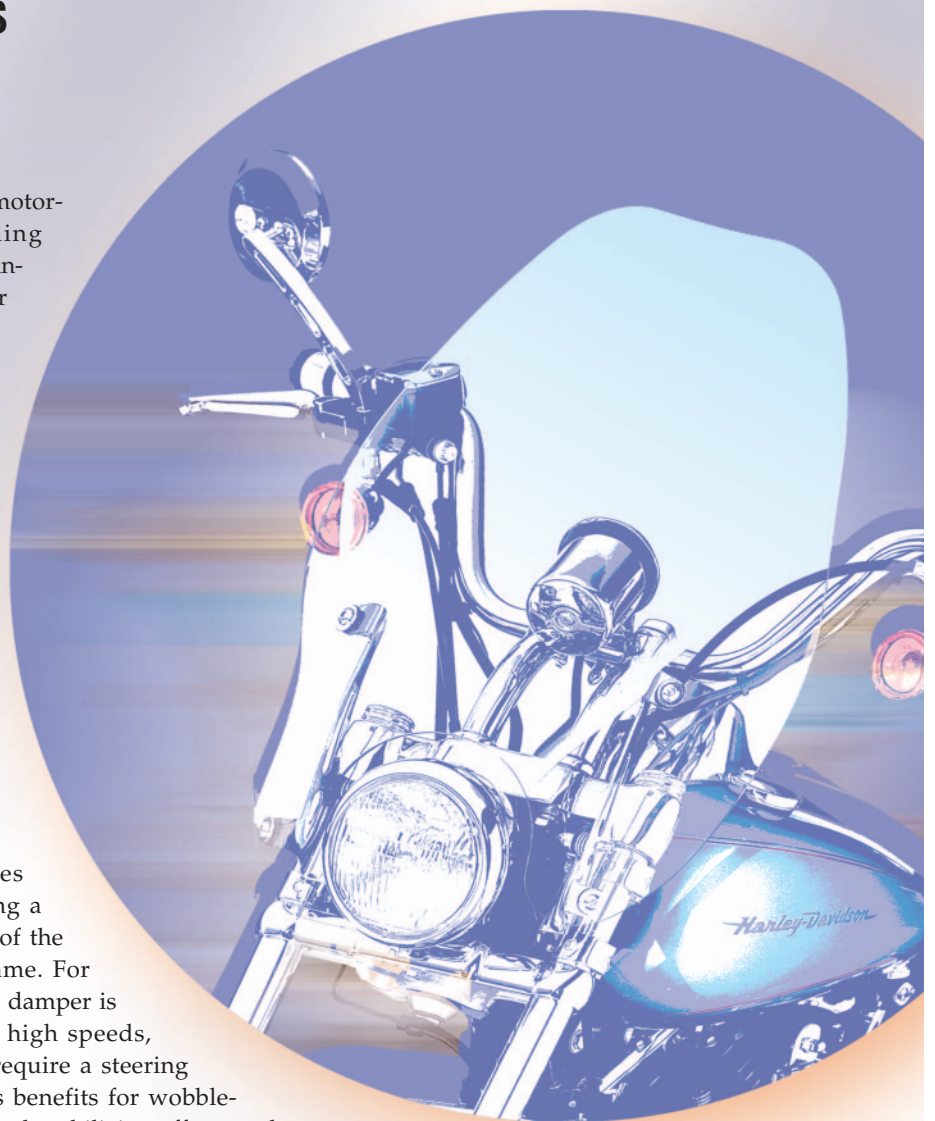
SIMOS EVANGELOU, DAVID J.N. LIMEBEER, ROBIN S. SHARP, and MALCOLM C. SMITH

## PASSIVE MECHANICAL COMPENSATORS INCORPORATING INERTERS

**A**dvances in modeling bicycle and motorcycle dynamics are providing improved understanding of the principal modes of motion under straight-running and steady-state cornering conditions; see, for example, [1] and the references therein. These studies show that under certain operating conditions, some of the machine's modes can be lightly damped or even unstable. The most important of these modes are wobble and weave. Wobble is a steering oscillation that is reminiscent of the caster shimmy that occurs in the front wheels of a supermarket cart, while weave is a fishtailing-type motion involving roll and yaw. The frequency of the wobble mode is of the order 8 Hz, while the weave frequency is about 3 Hz, where the exact figures depend on the speed and machine parameter values.

Modern high-performance motorcycles often employ a steering damper producing a moment that opposes the angular velocity of the steering assembly relative to the main frame. For machines with a stiff front frame, a steering damper is required to stabilize the wobble mode at high speeds, while older, more flexible machines may require a steering damper at intermediate speeds. Despite its benefits for wobble-mode performance, a steering damper has a destabilizing effect on the weave mode. As a result of this conflict, only a narrow range of damper coefficient values may be usable [2], [3].

Establishing damper settings that provide an optimal compromise between wobble- and weave-mode damping is an issue of considerable interest and is a focus of the present article.



© HARLEY-DAVIDSON® 2001 DIGITAL PRESS KIT

In particular, we replace the conventional steering damper with a network of interconnected mechanical components that retains the virtue of the damper, while improving the weave-mode performance. The improved performance is due to the fact that the network introduces phase compensation between the relative angular velocity of the steering system and the resulting steering torque.

The approach described here is underpinned by classical passivity ideas from circuit theory [4] as well as analogies between electrical and mechanical networks [5]; see “Passive Circuit Synthesis.” In the standard electrical-mechanical current-force analogy, an inductor corresponds to a spring, while a resistor represents a damper. To complete this analogy, a mechanical component is needed to

## Passive Circuit Synthesis

One of the principal motivations for the introduction of the inerter in [5] is the synthesis of passive mechanical networks. The fact that the mass element, together with the spring and damper, is insufficient to realize the totality of passive mechanical impedances can be seen using the force-current analogy between mechanical and electrical circuits. In this analogy, force and current are the through variables and velocity and voltage are the across variables. Moreover, the terminals of mechanical and electrical elements are in one-to-one correspondence. For the mechanical elements, the spring and damper have two independently movable terminals, whereas the terminals of the mass are its center of mass and a fixed point in an inertial frame (mechanical ground). The mass is therefore analogous to a grounded capacitor. In contrast, the inerter is a two-terminal device, analogous to an ungrounded capacitor, with both terminals freely and independently movable.

Figure A shows a table of element correspondences in the force-current analogy with the inerter replacing the mass element. The admittance  $Y(s)$  is the ratio of through to across quantities, where  $s$  is the standard Laplace transform variable. For mechanical networks in rotational form, the through and across variables are torque and angular velocity, respectively. It should be mentioned that the reciprocal definition of admittance for mechanical elements is commonly found in the literature, for example in [7], [8], and [25]. For further background on network analogies, see [5], [24], and [26].

The theory of passive circuits has been widely studied in the electrical engineering literature [4], [27]. A linear time-invariant two-terminal network that possesses a real rational impedance or admittance function is passive if and only if the impedance or admittance is positive real; see [4] and [27]. A celebrated result in electrical circuit synthesis, proved by Bott and Duffin, says that a rational, positive real function can be realized as the driving-

point impedance or admittance of a network comprised of only resistors, capacitors, and inductors [28]. The result can be translated over to the mechanical setting as follows [5].

### THEOREM

Let  $Y(s)$  be a positive-real rational function. Then there exists a two-terminal mechanical network that consists of a finite interconnection of springs, dampers, and inerters and whose admittance equals  $Y(s)$ .

This result allows the optimization of system properties without fixing the network structure in advance. For example, it can be shown [3] that the biquadratic real rational function

$$Y(s) = \frac{a_2 s^2 + a_1 s + a_0}{d_2 s^2 + d_1 s + d_0},$$

where  $a_2, a_1, a_0, d_2, d_1, d_0$  are nonnegative and at least one of  $d_0, d_1, d_2$  is positive, is positive real if and only if

$$a_1 d_1 \geq (\sqrt{a_0 d_2} - \sqrt{d_0 a_2})^2.$$

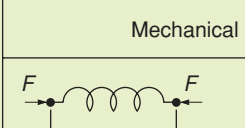
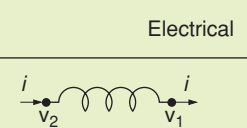
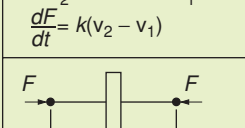
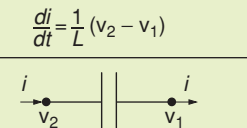
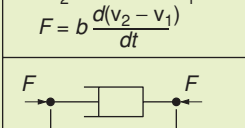
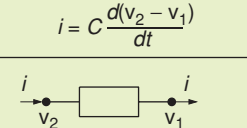
Mechanical		Electrical	
 $Y(s) = \frac{k}{s}$ Spring $\frac{dF}{dt} = k(v_2 - v_1)$	 $Y(s) = \frac{1}{Ls}$ Inductor $\frac{di}{dt} = \frac{1}{L}(v_2 - v_1)$		
 $Y(s) = bs$ Inerter $F = b \frac{d(v_2 - v_1)}{dt}$	 $Y(s) = Cs$ Capacitor $i = C \frac{d(v_2 - v_1)}{dt}$		
 $Y(s) = c$ Damper $F = c(v_2 - v_1)$	 $Y(s) = \frac{1}{R}$ Resistor $i = \frac{1}{R}(v_2 - v_1)$		

FIGURE A Electrical and mechanical circuit symbols and correspondences. In the force-current analogy, forces substitute for currents, and velocities substitute for voltages. The admittance  $Y(s)$  maps velocity and voltage into force and current, respectively.

represent a capacitor. Although a mass is analogous to a capacitor with one terminal grounded, a new device is required to represent a capacitor in general. The suitable masslike element is the inerter [5], which can be either a translational or rotational device.

In its rotational form, the inerter generates a resisting moment  $M$  between two hinged bodies that is proportional to the relative angular acceleration between them. Mathematically,

$$M = b(\dot{\omega}_1 - \dot{\omega}_2),$$

where  $\omega_1$  and  $\omega_2$  are the angular velocities of the bodies, and  $b$  is the inertance in  $\text{kg}\cdot\text{m}^2$ . As in [5], this use of the term inertance is consistent with its usage in acoustics [6] but is the reciprocal of the traditional usage in mechanical vibrations [7], [8], where it represents a transfer function from force to acceleration and is synonymous with the term acceleration in that field.

In control systems terms the inerter is used to produce phase lead. The effect of the inerter, which contains a flywheel of modest mass and dimensions, is amplified by high-ratio gearing. This gearing can be realized by an epicyclic arrangement [9] or by a harmonic drive [10]. It is possible to generate high inertance values with relatively low-mass components. More information about the mechanical synthesis of inerters can be found in "Inerter."

### MOTORCYCLE MODEL

The motorcycle model used in this article is based on the Suzuki GSX-R1000, a stiff-framed high-performance production vehicle. This motorcycle is fitted with a standard telescopic front fork suspension system and a swinging-arm-based rear suspension that incorporates a single spring-damper unit linked mechanically to the swing-arm, a monoshock suspension; see Figure 1.

In Figure 1, each constituent mass is represented by a red disk of diameter proportional to the corresponding mass. The model has a tree structure, except for one kinematically closed loop, which is associated with the monoshock description. The freedom associated with each body is shown in Figure 2. The symbolic multibody software system AUTOSIM [11] is used to assist the model-building process.

A detailed description of the model and its parameter set can be found in [12]; only a summary is given here. The main frame, which is allowed unrestricted motion, is pin connected to the steering system, the rider's upper body, and the rear swing-arm. The torsional compliance of the frame near the steering head is modeled by including a twist degree of freedom; this twist occurs about an axis that is perpendicular to the steer axis. The lower part of the front forks and the front wheel are free to translate along the fork line.

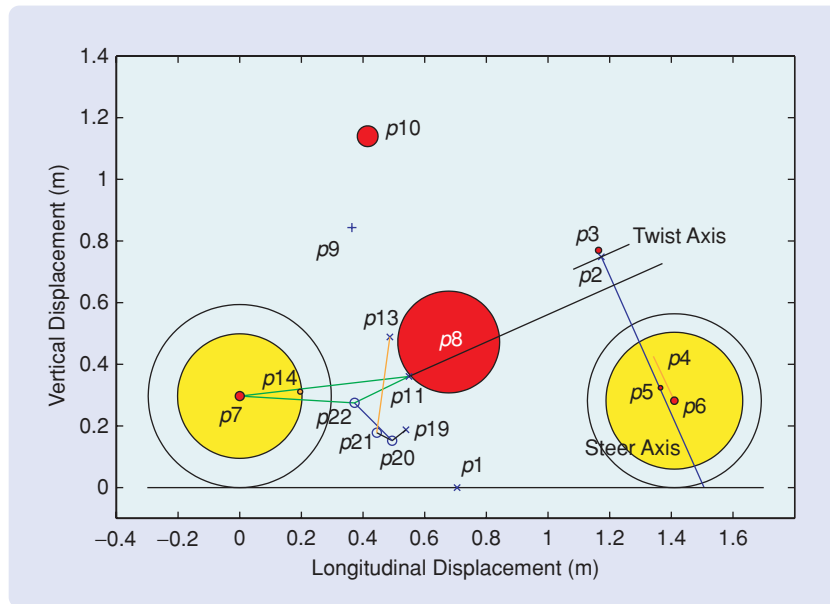


**FIGURE 1** Schematic of the GSX-R1000 motorcycle model. The scaled motorcycle and rider model shows the machine layout with each mass depicted as a proportionally scaled red disk. The motorcycle is shown in its nominal configuration with key points used in the multibody description labeled as  $p$ .

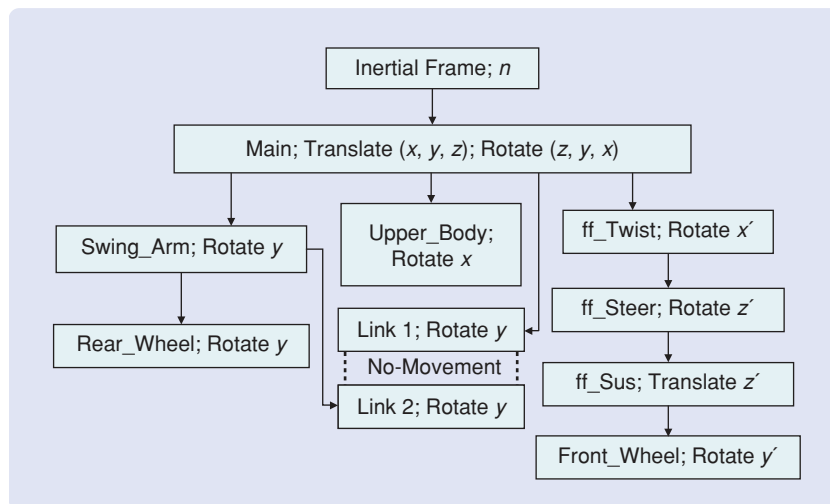


**FIGURE 2** Model parent-child kinematic dependencies [15]. The machine and rider multibody hierarchy show the relevant bodies and their degrees of freedom. Reference axis directions accord with SAE vehicle dynamics standards [16].

## Inerter

The inerter is a two-terminal device with the property that an equal and opposite force applied at the terminals is proportional to the relative acceleration between them. Mathematically, the inerter obeys the force-velocity law  $F = b(\dot{v}_1 - \dot{v}_2)$ , where the constant of proportionality  $b$  is called the inertance and has the units of kilograms. In its rotational form, the inerter obeys a moment-angular velocity law  $M = b(\dot{\omega}_1 - \dot{\omega}_2)$ ; in this case the inertance is measured in  $\text{kg}\cdot\text{m}^2$ . To be practically useful, the device must have a small mass. Also, the device must have reasonable overall dimensions and must be able to function in all spatial orientations.

One way in which a translational inerter can be constructed is illustrated in Figure B. The device comprises a rack-and-pinion mechanism, with the rack constrained to translate relative to the housing. For such devices the value  $b$  of the inertance is easy to compute in terms of the gear ratios and the flywheel's moment

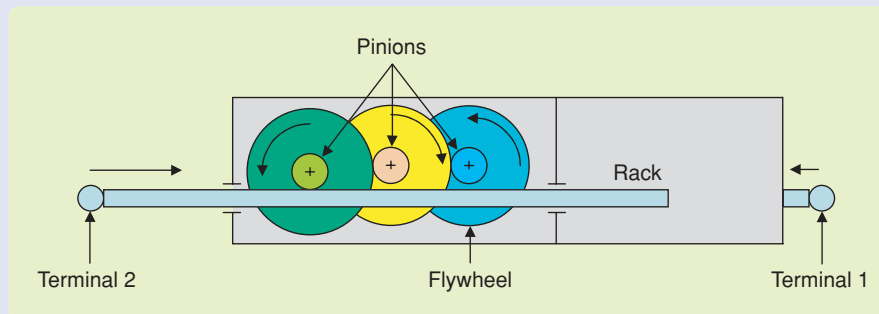


**FIGURE B** Schematic of the inerter principle. A rack and pinion gearing arrangement drives a rotating flywheel; the device's inertance is a function of the gear ratio and the flywheel inertia.

of inertia [5]. In general, if the device gives rise to a flywheel rotation of  $\alpha$  radians per meter of relative displacement between the terminals, then  $b = J\alpha^2$ , where  $J$  is the flywheel's moment of inertia and the remaining inertial effects are neglected. For a rotational inerter in which there is a gear ratio of  $n$  between rotations of the terminals and a flywheel with moment of inertia  $J$ , it follows that  $b = Jn^2$ . Several prototype devices according to [9] have been built and tested in the Engineering Department of Cambridge University; see for example figures C and D.



**FIGURE C** A prototype inerter. This translational inerter employs a ballscrew to convert the linear motion of the plunger into rotational motion of the flywheel (not shown). The device has a mass of approximately 1 kg and an inertance in the range 60–200 kg depending on the size of the flywheel. The device was designed by N.E. Houghton and manufactured in the Cambridge University Engineering Department.



**FIGURE D** Prototype motorcycle steering compensator. This rotational device employs an epicyclic gear box connected to a flywheel through a fluid coupling to realize a series inerter-damper. The mass is approximately 1.5 kg, while the inertance and damping are approximately 0.25  $\text{kg}\cdot\text{m}^2$  and 10  $\text{N}\cdot\text{m}\cdot\text{s}/\text{rad}$ , respectively. The device was designed by N.E. Houghton and manufactured in the Cambridge University Engineering Department.

Each road wheel is axisymmetric and is allowed to spin. Each tire is represented as having a finite width, and the ground contact points are allowed to migrate both circumferentially and laterally. This migration process is modeled by viewing the lowest point on each tire as the center of the road-tire contact patch. The motion states of the tire contact centers, the compression of the tires from their

nominal static equilibrium states, and the wheel camber angles are used in magic formula tire models [1], [12], [13] to compute the forces and aligning moments generated by the tires. Magic formula methods comprise empirical formulas and parameters that describe the forces and moments developed, as measured in laboratories, as functions of the operating conditions. Important operating

**Wobble is a steering oscillation that is reminiscent of the caster shimmy that occurs in the front wheels of a supermarket cart, while weave is a fishtailing-type motion involving roll and yaw.**

variables include the normal load, longitudinal and lateral slip, and wheel camber (or inclination) angle. As a result of the lateral compliance of the tires' carcasses, lateral force and moment variations are not generated instantaneously. The time constants associated with the force and moment production process or, more precisely, the relaxation lengths, are functions of speed [14]. The suspension springs and dampers are treated as linear, although suspension and steering limit stops are included.

Two feedback controllers are used in the model. The first is a fixed-gain proportional-plus-integral speed controller that generates the rear-wheel drive torque. The second is a speed-adaptive proportional-integral-derivative steering torque controller that responds to the lean angle error. With the aid of these controllers, the machine can track prescribed speed and lean-angle trajectories and, in particular, can be run to any feasible trim state to determine equilibrium configurations. The controller gains are set to zero for the uncontrolled motorcycle.

The AUTOSIM model file can be configured in a linear or nonlinear format. In the nonlinear configuration, a numerical simulation program for studying transient

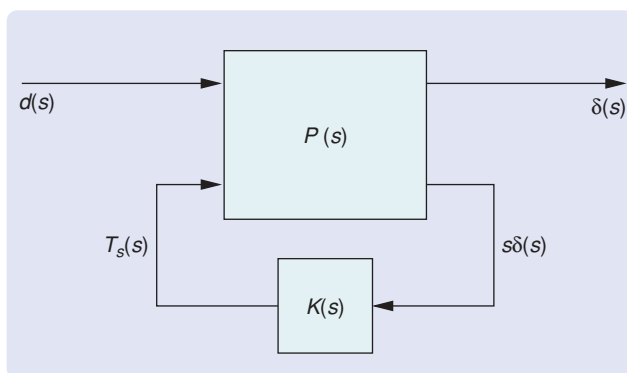


**FIGURE 3** Linearized motorcycle model and steering compensator. The linearized motorcycle model is denoted  $P(s)$ , while the steering compensator is shown as  $K(s)$  in the feedback loop. The input  $d(s)$  represents vertical road-displacement forcing, while the output  $\delta(s)$  is the steering angle and  $T_s(s)$  is the steer torque. The road forcing signal, which is a scalar variable, is applied to both wheels. The rear-wheel forcing signal is a delayed version of that at the front; the time delay is given by  $\tau = w/v$  in which  $w$  is the wheelbase and  $v$  is the forward speed. The steering compensator  $K(s)$  is constant in the case of a conventional steering damper.

machine behavior, or evaluating the machine's trim states, is obtained. Once a trim condition is reached, disturbances such as road profiling can be introduced. When the model is configured in its linear mode, the system is symbolically linearized for small perturbations about a general trim condition. The linearized models generated by AUTOSIM take a state-space form and a MATLAB M file is produced. Each

of the state-space matrices is parameterized to correspond to the trim condition being studied. The symbolic MATLAB file can be used to generate standard plots such as Nyquist and root locus diagrams.

When modeling the motorcycle in a conventional manner, the steering damper is included as an integral part of the machine. This normally low-profile component generates a steering torque that is proportional to steering velocity. To allow a more general relationship between the steering torque and the steering velocity, the steering damper is separated from the remainder of the system and represented as an external feedback loop as shown in Figure 3 [2], [3], [17]. The nominal motorcycle-damper combination will be referred to as the *standard* machine, while the motorcycle without a steering damper will be referred to as the *basic* machine. A conventional steering damper is represented as a pure gain in Figure 3. More general mechanical

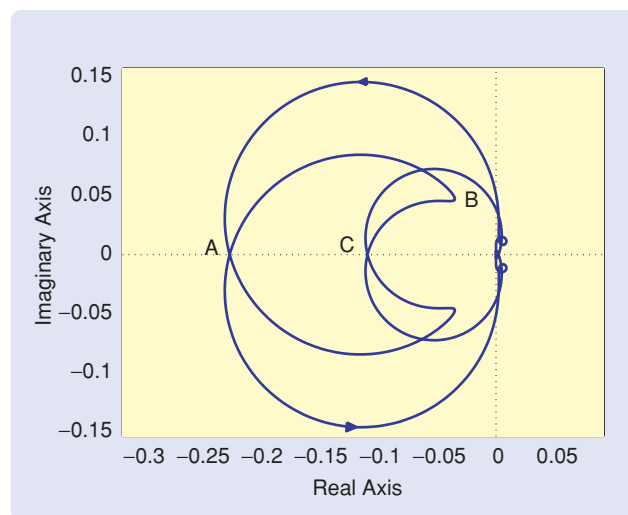


**FIGURE 4** Nyquist diagram of the straight-running basic machine. The diagram corresponds to the single-loop system with steering torque as input and with steering system angular velocity as output; the machine's forward speed is 75 m/s. The frequency associated with crossing point A, the wobble-mode resonant frequency, is 47.6 rad/s. The frequency associated with the cusp B is 33.8 rad/s, and that at crossing point C, the weave-mode resonant frequency, is 28.4 rad/s. If the damper coefficient is selected so that the point  $-1/c$  is at A, the motorcycle oscillates at the wobble-mode frequency. If the damper coefficient is selected so that the point  $-1/c$  is at C, the machine oscillates at the weave-mode frequency.

networks are represented by  $K(s)$  in which  $s$  is the Laplace variable. The transfer function  $K(s)$  from angular velocity to torque is called the admittance function of a mechanical network following the convention of [24, pp. 45, 46, 326] but in contrast to other uses in mechanical engineering [6, p. 238] and [8, p. 207].

### CHARACTERISTICS OF THE NEAR-STANDARD MACHINE

Figure 4 shows a Nyquist diagram of the linearized model of the basic machine in a straight-running equilibrium condition at 75 m/s. This diagram can be used to study the effect of changing the steering damper coefficient. The model has two right-half-plane poles for this operating condition because the wobble mode is unstable. Since the steering damper is represented as a pure gain in the feedback loop of Figure 3, it follows from the Nyquist criterion that stability of the standard machine requires two counterclockwise encirclements of the point  $-1/c$ , where  $c$  is the steering damper constant. If the steering damping is set at a low value such that the point  $-1/c$  is located at *A*, the machine is on the stability boundary and thus oscillates at 47.6 rad/s, which is the wobble-mode frequency. If the steering damping is now increased, two counterclockwise encirclements of the point  $-1/c$  result, and the motorcycle is stable. If the steering damping is increased further so that the point  $-1/c$  coincides with *C*, the machine oscillates at 28.4 rad/s and the weave mode is on the stability boundary. Further increases in the steering damping render the machine unstable since the point  $-1/c$  is not encircled. The nominal steering damper coefficient is 6.944 N-m-s/rad, thereby locating the point  $-1/c$  at  $-0.144$ , which is approximately midway between *A* and *C*.

When the speed increases from 75 m/s to 85 m/s, the interval on the negative-real axis associated with stabilizing damper parameter values moves to the left [3]. This shift moves the weave-mode crossing point toward the point  $-1/c$  associated with the nominal damping coefficient, and the wobble-mode crossing point moves away from it. As a result, this speed increase reduces the weave-mode damping factor and increases the wobble-mode damping factor.

Figure 5 shows straight-running root loci where speed is the varied parameter. When the steering damper coefficient is reduced from its nominal (standard machine) value, the wobble mode becomes unstable at high speed, while the high-speed weave-mode damping increases.

The damper has almost no influence on the frequency (imaginary part) associated with either of these modes.

Replacing the damper with an inerter, for which  $K(s) = bs$ , leads to the root locus diagram of Figure 6.

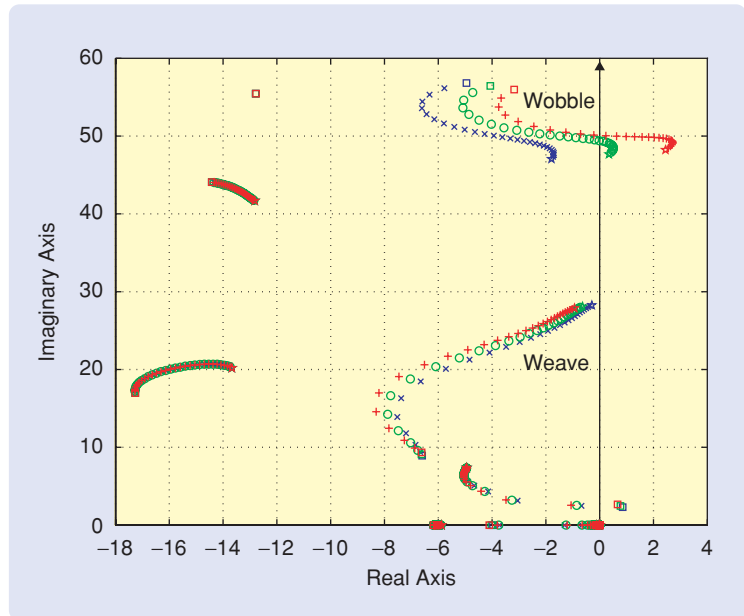


**FIGURE 5** Influence of the steering damper on the root loci of the straight-running motorcycle. Speed, which is the varied parameter, is increased from 5 m/s ( $\square$ ) to 75 m/s ( $\star$ ). The  $\times$  locus is associated with the nominal machine damping value of 6.944 N-m-s/rad, the  $\circ$  locus is associated with a steering damping value of 3.94 N-m-s/rad, and the  $+$  locus with a steering damping value of 0.94 N-m-s/rad.

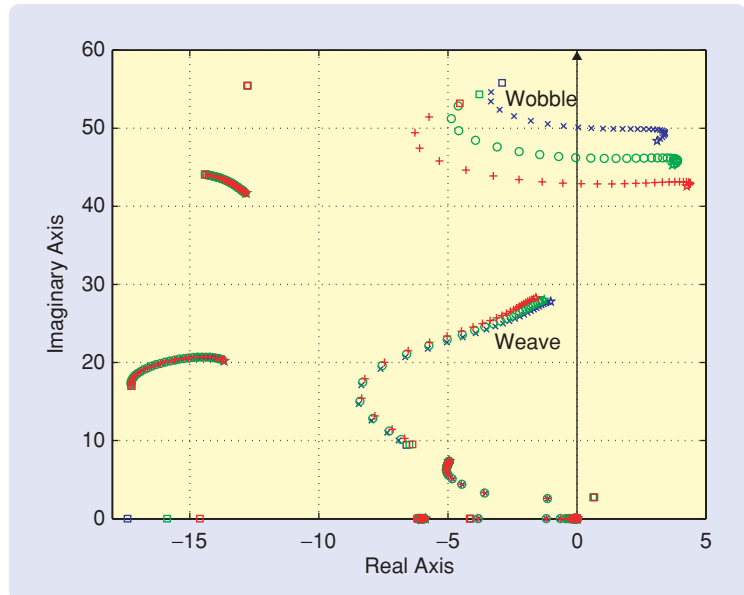


**FIGURE 6** Influence of a steering inerter on the root loci of the straight-running motorcycle. Speed, which is the varied parameter, is increased from 5 m/s ( $\square$ ) to 75 m/s ( $\star$ ). The  $\times$  locus is associated with the basic machine, the  $\circ$  locus represents the basic machine fitted with a steering inertance of 0.1 kg-m<sup>2</sup>, and the  $+$  locus represents the basic machine fitted with a steering inertance of 0.2 kg-m<sup>2</sup>.

**The dynamic characteristics of high-performance motorcycles can be improved by replacing the conventional steering damper with a passive mechanical steering compensator.**

Although the inerter stabilizes the weave mode at high speeds, it has a detrimental effect on the wobble-mode damping. The reduction in the wobble-mode frequency is caused by the effective increase in the steering system's moment of inertia. With regard to the damping of the weave and wobble modes, the inerter and damper introduce opposite trends.

**COMPENSATION NETWORK**

**Desired Network Properties**

The results of the previous section suggest that a mechanical network that is damper-like over the wobble-mode frequency

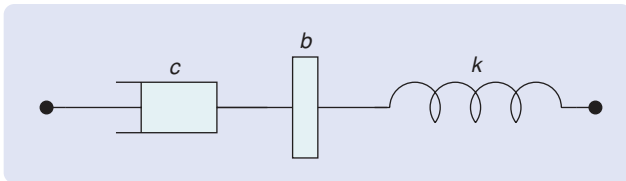


**FIGURE 7** Series resonant filter. This series connection of a damper, inerter, and spring, constituting a resonant filter, provides frequency-localized damping influence.

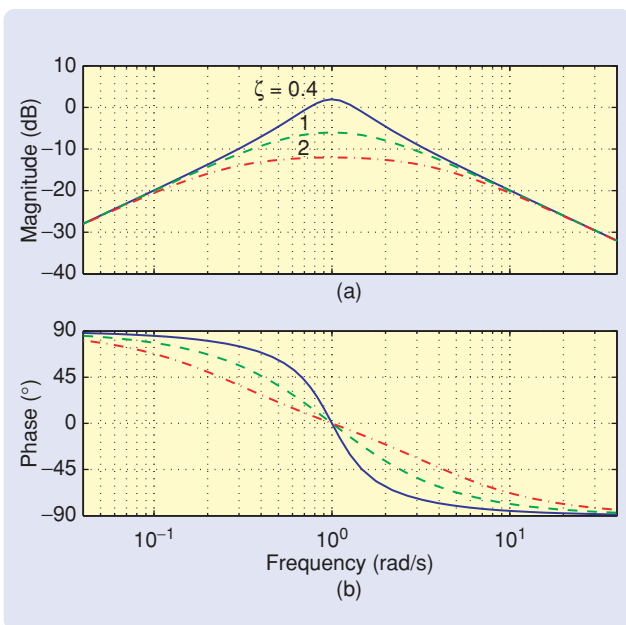


**FIGURE 8** Frequency-response characteristics of the series resonant filter network with the resonant frequency normalized to  $\omega_n = 1$ . Three values of damping ratio  $\zeta$  are illustrated.

range (5–9 Hz) and inerter-like at the lower frequencies associated with the weave mode (2–3 Hz) might be beneficial. Over the still lower frequency range used by the rider (0–0.5 Hz) [19], [20], for balancing and path-following control, the network must be high pass to allow unhindered rider steering action. Spring-like properties are undesirable as are high values of steady-state gain.

It can be shown that the series connection of an inerter and damper has the admittance function  $scb/(sb + c)$ , where  $b$  and  $c$  are the inertance and damping coefficient respectively. The frequency response of this admittance function is similar to that of an inerter (respectively, damper) at frequencies below (respectively, above) the break frequency  $c/b$ . This frequency response function can be beneficial for simultaneous control of wobble and weave. A related network is the resonant filter consisting of the series connection of a damper, an inerter and a spring (see Figure 7). This network has the admittance

$$Y(s) = \frac{s}{s^2 + sk/c + k/b}, \quad (1)$$

where  $b$ ,  $c$ , and  $k$  denote the inertance, damping coefficient, and spring stiffness, respectively.

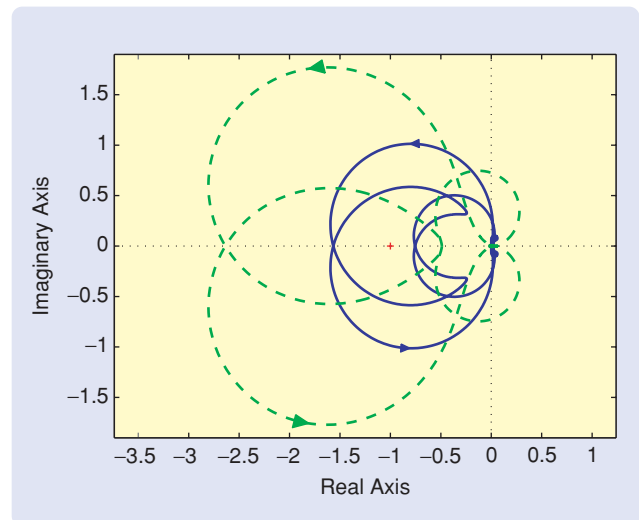


**FIGURE 9** Nyquist diagram of the straight-running motorcycle with a forward speed of 75 m/s. The solid line represents the standard machine, while the dashed line corresponds to the compensated system using the series resonant filter shown in Figure 7 with design values  $\omega_n = 50$  rad/s,  $\zeta = 0.4$ , and  $k = 500$  N-m/rad.

## Frequency Response Design

It is instructive to develop initial design guidelines for the network parameters using classical frequency-response ideas. The network admittance (1) can be rewritten in the form

$$Y(s) = k \frac{s}{s^2 + 2\zeta\omega_n s + \omega_n^2},$$

in which

$$\omega_n = \sqrt{k/b}, \quad \zeta = \frac{\sqrt{bk}}{2c}. \quad (2)$$

It can be seen from the frequency-response characteristics of the network shown in Figure 8 that this network acts like an inerter at low frequencies and introduces damping in the vicinity of  $\omega_n$ , which must be tuned to the wobble-mode frequency. The damping ratio  $\zeta$  is a design parameter that determines the sharpness of the magnitude peak and the rate of change of phase with frequency. Smaller values of  $\zeta$  give a more rapid transition from *inertlike* to *dampertlike* behavior. Larger values of  $\zeta$  provide a wider range of frequencies where *dampertlike* behavior persists. The peak value of the magnitude characteristic is achieved at  $\omega_n$  and takes the value of  $c$ , the damper constant. It can be seen in (2) that  $\omega_n$  and  $\zeta$  fully specify the phase characteristics of the network.

For an initial trial design the parameters  $\omega_n = 50$  rad/s and  $\zeta = 0.4$  are selected. Prior to fixing a value of the spring constant, it is observed that  $k = 320$  N-m/rad places the point  $-1$  in the middle of the stable  $k$ -value range in the 75 m/s straight-running condition. However, since this value of  $k$  does not produce adequate wobble-mode damping performance at high lean angles, the spring stiffness is increased to  $k = 500$ . This change improves the wobble-mode damping globally but at the expense of the weave mode. Back substitution gives inerter and damper parameter values of  $b = 0.2$  kg-m<sup>2</sup> and  $c = 10$  N-m-s/rad, respectively. The influence of this particular choice of parameters is illustrated in Figure 9. It may be observed that the network moves the negative-axis crossing point associated with weave-mode instability toward the origin and the crossing point linked to wobble to the left of the diagram. The network opens up the interval over which two counterclockwise encirclements can be achieved. The root locus plot that results from this mechanical network with parameter values  $b = 0.2$  kg-m<sup>2</sup>,  $c = 10$  N-m-s/rad, and  $k = 500$  N-m/rad is shown in Figure 10. Although the design is based on a single high-speed straight-running linearized model, compared with the standard machine, substantial improvements in the damping of both the

wobble and the weave modes under all operating conditions are achieved. The improvement in the high-roll angle (45°) case is worthy of particular note [3].

## OPTIMIZATION

We now optimize the parameters of the series resonant filter. The chosen performance criterion reflects the role played by road-displacement disturbances in stability-related road traffic accidents [21] in the form of an  $\mathcal{H}_\infty$  response measure, together with a penalty on the closeness of approach of the open-loop Nyquist locus to the point  $-1$ .

The objective function considered is

$$J_f = \max_{\Omega} \{\max\{J_1, \gamma J_2\}\}, \quad (3)$$

where

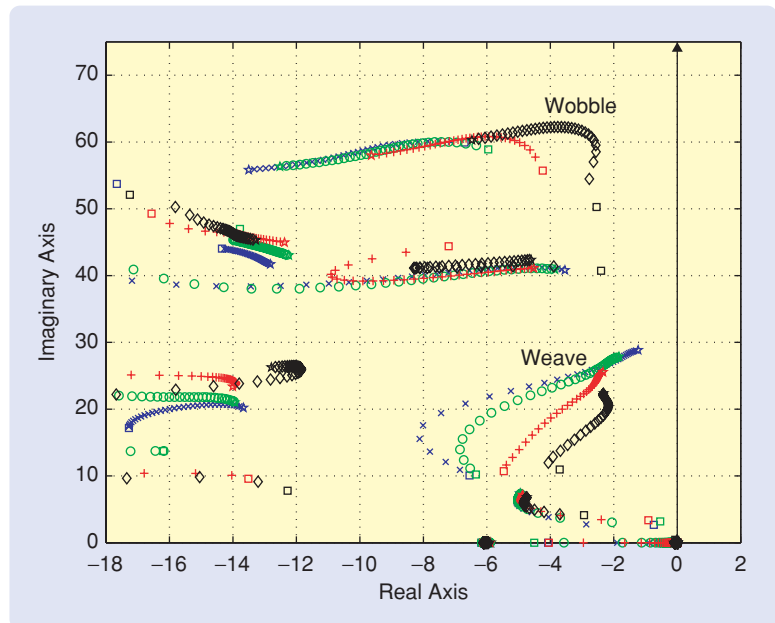


**FIGURE 10** Root loci for the compensated motorcycle. Four values of roll angle are illustrated: straight running ( $\times$ ), 15° ( $\circ$ ), 30° ( $+$ ), and 45° ( $\diamond$ ). The speed is varied from 7 m/s ( $\square$ ) to 75 m/s ( $*$ ). The machine is fitted with the series resonant network with the parameter values  $b = 0.2$ ,  $c = 10$ , and  $k = 500$ .

**TABLE 1** Design parameters, objective functions, and worst-case configurations obtained by optimizing the frequency-domain index (3) for the conventional steering damper and the series resonant filter.

Compensator	Parameters	$J_f$	Maximum		
			deg	m/s	rad/s
Conventional damper	$c = 8.0695$	109.8412	45	9	52.97
Series resonant filter	$k = 594.08$ $c = 13.716$ $b = 0.24252$	40.576	45	7	49.95



$$J_1 = \max_{\omega_i} \left| \frac{P_{11}(j\omega_i)}{1 - K(j\omega_i)P_{22}(j\omega_i)} \right| \quad (4)$$

and

$$J_2 = \max_{\omega_i} \left| \frac{1}{1 - K(j\omega_i)P_{22}(j\omega_i)} \right|. \quad (5)$$

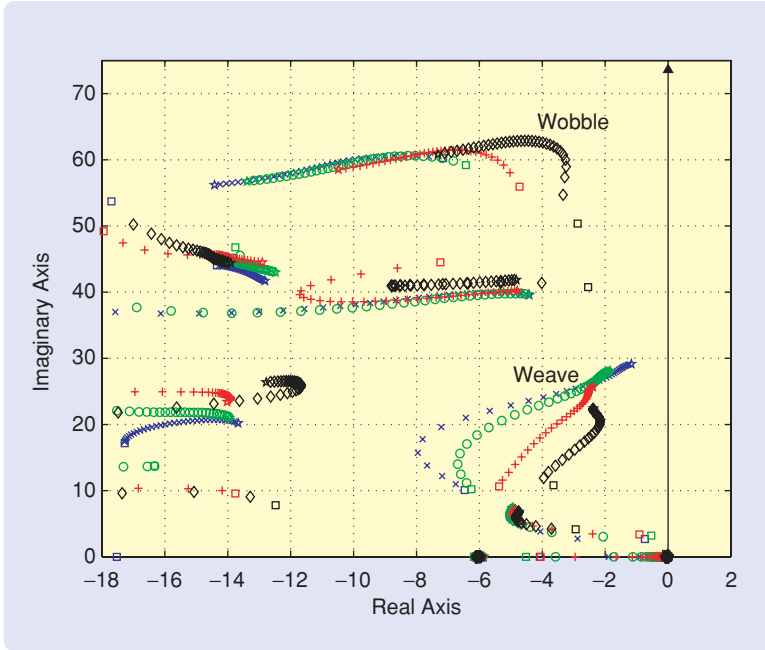


**FIGURE 11** Root loci for the motorcycle compensated by the optimized series resonant filter with parameters as in Table 1. Four values of roll angle are illustrated, namely, straight running ( $\times$ ),  $15^\circ$  ( $\circ$ ),  $30^\circ$  ( $+$ ), and  $45^\circ$  ( $\diamond$ ). The speed is varied between 7 m/s ( $\square$ ) and 75 m/s ( $\star$ ).

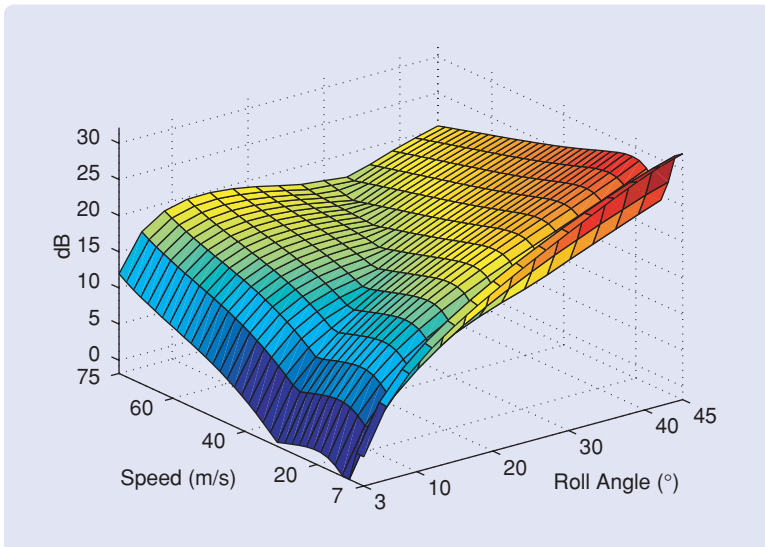


**FIGURE 12** Road-forcing gain as a function of operating condition. The speed is varied between 7 and 75 m/s, and the roll angle between  $3^\circ$  and  $45^\circ$ . The motorcycle is fitted with the frequency-response-optimized series resonant compensation network.

The set  $\Omega$  of linear motorcycle models used in (3) contains linearized models corresponding to trim roll angles of  $0, 3, 6, \dots, 45^\circ$  and trim speeds of  $7, 9, 11, \dots, 75$  m/s. The subindex  $J_1$  in (4) is reminiscent of the  $\mathcal{L}_\infty$ -norm of the transfer function between road-displacement forcing and steer angle (see the “Motorcycle Model” section and Figure 3), while  $J_2$  in (5) is the reciprocal of the distance of closest

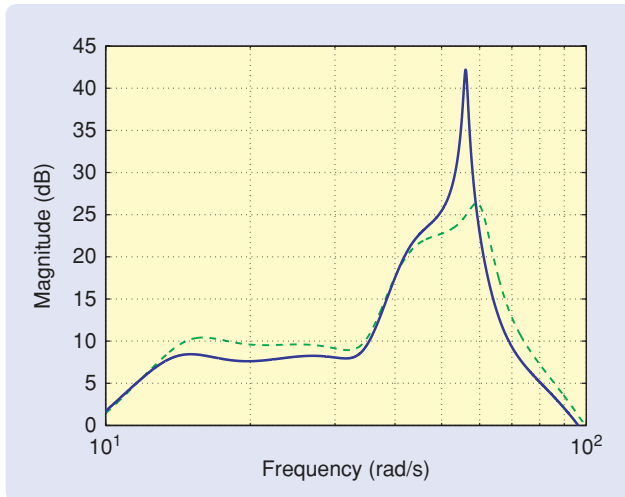
approach between the Nyquist locus and the point  $-1$ .  $J_2$  effectively penalizes high values of the classical sensitivity function [22]. The subindex  $J_2$  is weighted in  $J_f$  by the constant  $\gamma$ , set by trial to a value 16. When evaluating  $J_f$ , a 100-point angular frequency sequence in geometric progression, from  $\omega = 10^{1.3}$  rad/s to  $\omega = 10^{1.85}$  rad/s is used; this range includes all of the peaks in  $J_f$ . The MATLAB sequential quadratic programming algorithm `fmincon` [23] is used for optimization. The algorithm is initialized using the parameters obtained from the results described in the “Frequency Response Design” section.

## RESULTS

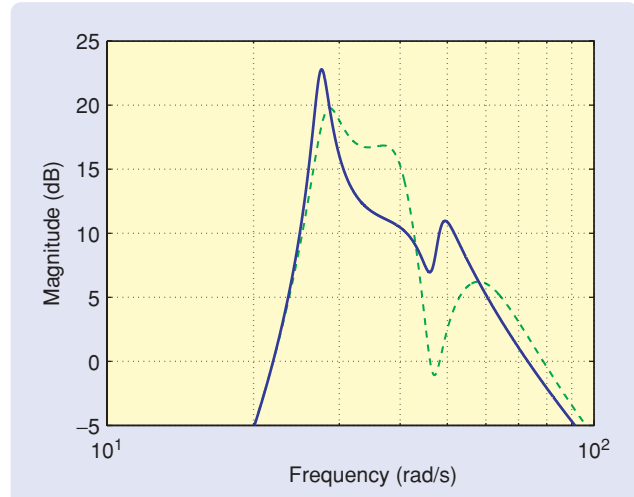
The results of optimizing with the frequency response index (3) are given in Table 1 for the conventional damper and the series resonant filter. In addition to the optimal parameter values, the table provides the minimum values achieved for  $J_f$ , the trim condition at which the minimum is achieved, and the worst-case frequencies associated with the limiting value of the index. The wobble mode dictates the lowest achievable value of  $J_f$ . For the filter, the closest approach between the Nyquist plot and the point  $-1$  exceeds  $16/40.576 = 0.394$ , where 16 is the value of  $\gamma$  used in (3).

Figure 11 shows the root locus of the motorcycle’s key modes for a wide range of speeds and roll angles using the optimized series resonant filter network. The network achieves improved damping ratios for each of the machine’s lightly damped modes.

Figure 12 shows the road-forcing response  $J_1$  in (4) with the optimized series resonant filter network installed; the trim state ranges over the motorcycle’s operating regime. As expected, under straight-running conditions, the road-forcing response is zero. In common with each of the other networks, the highest gain values, which occur at low speeds and high roll angles, correspond to the excitation of the wobble mode. High values of road-forcing-to-steer-angle gain also occur under high-speed, low-roll-



**FIGURE 13** Bode magnitude plot of steer angle response to road-displacement forcing (0 dB = 1 rad/m). The machine is operating at a forward speed of 15 m/s and a roll angle of 45°. The solid line represents the standard machine, while the dashed line represents the machine with the optimized series resonant filter network compensator.



**FIGURE 14** Bode magnitude plot of steer angle response to road-displacement forcing (0 dB = 1 rad/m). The machine is operating at a forward speed of 75 m/s and a roll angle of 15°. The solid line represents the standard machine, while the dashed line represents the machine with the optimized series resonant filter network compensator.

angle conditions (see 75 m/s and 15° roll angle), which correspond to excitation of the weave mode.

The road-forcing characteristics of the machine are also illustrated by the frequency-response plots shown in Figures 13 and 14. As is evident from the first of these figures, the series resonant filter network decreases the peak wobble-mode road-forcing gain by approximately 15 dB. For the trim condition considered in Figure 13, the wobble mode is particularly vulnerable to road-displacement forcing. Figure 14 corresponds to a high-speed trim condition in which the weave mode is correspondingly challenged. In this case, the network reduces the weave-mode peak by approximately 3 dB as compared to the standard machine.

## CONCLUSIONS

This article shows that the dynamic characteristics of high-performance motorcycles can be improved by replacing the conventional steering damper with a passive mechanical steering compensator. The steering compensators are mechanical networks comprising springs, dampers, and inerters. The compensators show the potential to significantly improve the damping of both wobble and weave modes simultaneously. These networks exploit the inverter's ability to provide phase advance. The compensator's role can be interpreted as that of a feedback element in a control systems structure, despite its consisting of passive mechanical elements.

The design methodology adopted uses Nyquist frequency response ideas, root-locus analysis, and loop-shaping design to obtain a preliminary choice of parameters, which are then refined by numerical opti-

mization. The results show substantial global performance improvements as compared with conventional steering dampers.

The broad issue of the practical implementation of passive mechanical compensators is the subject of ongoing research, including the fabrication of integrated mechanical networks as illustrated in Figure 7. Additional issues such as the selection of optimal gear ratios for the inerters and the correct dimensioning of the components so that they have sufficient working life are also important considerations. From a packaging perspective, a steering compensator needs to be acceptably small and light. Ideally, the compensator will fit in the space normally occupied by a conventional steering damper.

## AUTHOR INFORMATION

*Simos Evangelou* received the B.A./M.Eng. degree in electrical and information sciences from the University of Cambridge, United Kingdom, in 1999 and the Ph.D. degree in control engineering from Imperial College London, in 2004. In 2006 he was appointed a lecturer at Imperial College London, for the departments of mechanical and electrical and electronic engineering. Previously he worked as a research associate from 2004 to 2005. His research interests include the modeling, stability analysis and control of single-track vehicles, the application of control theory to mechanical systems, dynamic system modeling, and control systems theory.

*David J.N. Limebeer* (d.limebeer@imperial.ac) received the B.Sc. degree in electrical engineering from the University of Witwatersrand, Johannesburg, in 1974, the M.Sc. and Ph.D. degrees in electrical engineering from the University

of Natal, Durban, South Africa, in 1977 and 1980, respectively, and the D.Sc. degree from the University of London in 1992. He has been with Imperial College London, since 1984, where he is currently the head of the Department of Electrical and Electronic Engineering. He has published over 100 papers and a textbook on robust control theory. Three of his papers have been awarded prizes, including the 1983 O. Hugo Schuck Award. He is a past editor of *Automatica* and a past associate editor of *Systems and Control Letters* and the *International Journal of Robust and Nonlinear Control*. He is a Fellow of the IEEE, the IEE, the Royal Academy of Engineering, and the City and Guilds Institute. His research interests include control system design, frequency response methods, H-infinity optimization, and mechanical systems. He is qualified as an IAM senior motorcycle instructor and received a RoSPA certificate for advanced motorcycling. He can be contacted at Imperial College London, Department of Electrical and Electronic Engineering, Exhibition Road, London SW7 2AZ U.K.

**Robin S. Sharp** is professorial research fellow in the Department of Electrical and Electronic Engineering at Imperial College London. He is a member of the Dynamical Systems and Mechatronics Working Group of the International Union of Theoretical and Applied Mechanics, the editorial board of *Vehicle System Dynamics*, and the editorial advisory board of *Multibody System Dynamics*. He was first vice-president and secretary general of the International Association for Vehicle System Dynamics, editorial panel member and book review editor for *The Proceedings of the Institution of Mechanical Engineers, Journal of Mechanical Engineering Science, Part C*, and editorial panel member of *The Proceedings of the Institution of Mechanical Engineers, Part D, Journal of Automobile Engineering*. From 1990–2002, he was professor of automotive product engineering at Cranfield University. He was a visiting associate research scientist at the University of Michigan Transportation Research Institute, Ann Arbor. His research covers topics in automotive dynamics and control as well as in control and stability of single-track vehicles, unmanned air vehicles, and the application of optimal preview and learning control to road vehicle driving/riding.

**Malcolm C. Smith** received the B.A. (M.A.) degree in mathematics, the M.Phil degree in control engineering and operational research, and the Ph.D. degree in control engineering, all from the University of Cambridge, U.K. He was subsequently a research fellow at the German Aerospace Centre, a visiting assistant professor and research fellow with the Department of Electrical Engineering at McGill University, and an assistant professor with the Department of Electrical Engineering at the Ohio State University. In 1990 he returned to the University of Cambridge where he is currently a professor. He is a fellow of Gonville and Caius College. His research interests include

control system design, frequency response methods, H $\infty$  optimization, nonlinear systems, active suspension, and mechanical systems. He was a corecipient of the 1992 and 1999 George Axelby Outstanding Paper Awards, both times for joint work with Dr Tryphon T. Georgiou. He is a Fellow of the IEEE.

## REFERENCES

- [1] D.J.N. Limebeer and R.S. Sharp, "Bicycles, motorcycles, and models," *IEEE Control Syst. Mag.*, vol. 26, no. 5, pp. 34–61, 2006.
- [2] S. Evangelou, D.J.N. Limebeer, R.S. Sharp, and M.C. Smith, "Steering compensation for high-performance motorcycles," in *Proc. 43rd CDC*, Paradise Island, Bahamas, 14–17 Dec. 2004, pp. 749–754.
- [3] S. Evangelou, D.J.N. Limebeer, R.S. Sharp, and M.C. Smith, "Mechanical steering compensators for high-performance motorcycles," *J. Appl. Mech.*, to be published.
- [4] R.W. Newcomb, *Linear Multiport Synthesis*. New York: McGraw Hill, 1966.
- [5] M.C. Smith, "Synthesis of mechanical networks: The inerter," *IEEE Trans. Automat. Contr.*, vol. 47, no. 10, pp. 1648–1662, 2002.
- [6] C.L. Morfey, *Dictionary of Acoustics*. New York: Academic, 2001.
- [7] D.E. Newland, *Mechanical Vibration Analysis and Computation*. White Plains, NY: Longman, 1989.
- [8] D.J. Inman, *Engineering Vibration*, 2nd ed. Englewood Cliffs, NJ: Prentice Hall, 2001.
- [9] M.C. Smith, "Force-controlling mechanical device," patent pending, Int. pub. WO 03/005142, 4 July 2001, [Online]. Available: <http://v3.espacenet.com/textdoc?DB=EPODOC&IDX=WO03005142&F=0>
- [10] Harmonic drive. [Online]. Available: <http://www.hdsystemsinc.com>
- [11] *Autosim 2.5+ Reference Manual*, Mechanical Simulation Corp., Ann Arbor, MI, 1998 [Online]. Available: <http://www.carsim.com>
- [12] R.S. Sharp, S. Evangelou, and D.J.N. Limebeer, "Advances in the modeling of motorcycle dynamics," *Multibody Syst. Dynamics*, vol. 12, no. 3, pp. 251–283, 2004.
- [13] H.B. Pacejka, *Tyre and Vehicle Dynamics*. Oxford, U.K.: Butterworth Heinemann, 2002.
- [14] E.J.H. de Vries and H.B. Pacejka, "The effect of tyre modeling on the stability analysis of a motorcycle," in *Proc. AVEC'98*, Nagoya: SAE Japan, 1998, pp. 355–360.
- [15] R.S. Sharp, S. Evangelou, and D.J.N. Limebeer, "Multibody aspects of motorcycle modelling with special reference to autosim," in *Advances in Computational Multibody Systems*, J.G. Ambrósio, Ed. Dordrecht, The Netherlands: Springer-Verlag, 2005, pp. 45–68.
- [16] Society of Automotive Engineers, "Vehicle dynamics terminology," in *Proc. SAE J670e*, Warrendale, PA, 1976.
- [17] C. Papageorgiou and M.C. Smith, "Positive real synthesis using matrix inequalities for mechanical networks: Application to vehicle suspension," in *IEEE Trans. on Contr. Syst. Tech.*, vol. 14, no. 3, pp. 423–435, 2006.
- [18] R.C. Dorf and R.H. Bishop, *Modern Control Systems*. Englewood Cliffs, NJ: Prentice Hall, 2001.
- [19] A. Aoki, "Experimental study on motorcycle steering performance," *SAE paper 790265*, 1979.
- [20] M. Sugizaki and A. Hasegawa, "Experimental analysis of transient response of motorcycle rider systems," *SAE paper 881783*, 1988.
- [21] D.J.N. Limebeer, R.S. Sharp, and S. Evangelou, "Motorcycle steering oscillations due to road profiling," *J Appl. Mech.*, vol. 69, no. 6, pp. 724–739, 2002.
- [22] M. Green and D.J.N. Limebeer, *Linear Robust Control*. Englewood Cliffs, NJ: Prentice Hall, 1995.
- [23] The Mathworks Inc., *MATLAB 6 Reference Manual*, 2000 [Online]. Available: <http://www.mathworks.com>
- [24] J.L. Shearer, A.T. Murphy, and H.H. Richardson, *Introduction to System Dynamics*. Reading, MA: Addison-Wesley, 1967.
- [25] E.L. Hixson, "Mechanical impedance," in *Shock and Vibration Handbook*, 2nd ed., C.M. Harris and C.E. Crede, Eds. New York: McGraw-Hill, 1976, chap. 10.
- [26] A.G.J. MacFarlane, *Dynamical System Models*. London: Harrap, 1970.
- [27] B.D.O. Anderson and S. Vongpanitlerd, *Network Analysis and Synthesis*. Englewood Cliffs, NJ: Prentice Hall, 1973.
- [28] M.E.V. Valkenburg, *Introduction to Modern Network Synthesis*. New York: Wiley, 1960.

